THE JOURNAL OF PHYSICAL CHEMISTRY LETTERS
A JOURNAL OF THE AMERICAN CHEMICAL SOCIETY

pubs.acs.org/JPCL

Letter

Electric-Field-Induced Ion Migration Behavior in Methylammonium Lead Iodide Perovskite

Yu Du, Sushu Wan, Mingcai Xie, Yuren Xia, Weiqing Yang, Zhihong Wei, Yajie Zhu, Yan Hua, Zhong Jin, Daocheng Hong,* and Yuxi Tian*

Cite This: J. Phys. Chem. Lett. 2021, 12, 7106–7112

Read Online

ACCESS | Metrics & More | Article Recommendations | Supporting Information

ABSTRACT: Ionic movement inside organometal halide perovskites (OMHP) materials has been widely reported to be linked with stability issues in the perovskite-based optoelectronic devices. However, the dynamic processes of the ionic movement and how they influence the devices are still not well-understood. In this work, we applied an external electric field to the $CH_3NH_3PbI_3$ crystal and simultaneously monitored the PL behaviors. Two successive PL responses were observed in the same location of the crystal. First, an irreversible PL quenching was observed caused by the photo-annealing effect under an electric field accompanied by a permanent morphology change. The annealed area also showed reversible PL variation, which was attributed to the activation–deactivation of the radiative recombination centers induced by the migration of the iodine ions. Such results can help us gain a deep insight into how the ionic movements in OMHPs influence the performance of the perovskite-based optoelectronic devices under working conditions.

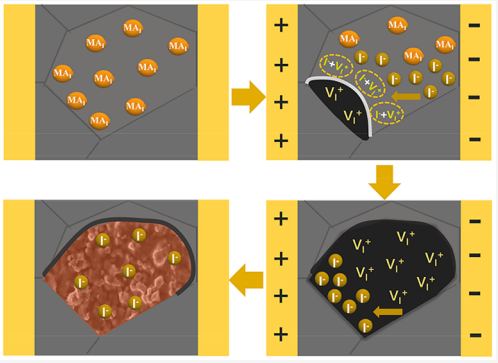

We have witnessed the skyrocketing progress of the performance of organometal halide perovskite (OMHP)-based optoelectronic devices during the past decade; for example, the energy conversion efficiency of perovskite solar cells has reached 25.5%.[1,2] Nevertheless, the unsatisfactory device stability[3,4] and current–voltage hysteresis[5−7] are still the main issues existing in most perovskite-based optoelectronic devices under operational conditions. For example, O'Regan et al. have observed current–voltage hysteresis phenomena in $CH_3NH_3PbI_3$-based solar cells when measuring the transient photovoltage and differential capacitance.[8] Miyano et al. also witnessed the influence of interface on the degradation of lead iodide perovskite by extending the time scale and the bias range in electronic measurements.[9] Most of these detrimental behaviors were thought to originate from the ion accumulation or migration effects in OMHPs.[10−14] Therefore, understanding what effects the mobile ions will bring to the perovskite materials is urgently required because it could provide hints for eliminating the negative aspects of OMHP materials when applied in optoelectronic devices.

Investigations on the effects of mobile ions have already been widely reported. Macroscopic migration of iodine ions in a $CH_3NH_3PbI_3$ film under an electric field was first experimentally observed by Yuan et al. and was recognized to be a result of solid-state chemical reactions.[15] PL inactive domains were also suggested to be correlated with the ion migration under an electric field at room temperature by many groups.[16−18] Kim et al. also confirmed that the doping of K^+ in perovskite crystals can effectively suppress the ion migration and passivate the nonradiative recombination centers.[19] In addition, the ionic migration will also cause the displacement of vacancies or influence the charge transport properties in perovskite materials according to related investigations.[20−22] However, the connection between ion migration and the properties of the perovskite materials still has not been definitively established.

In this work, to investigate the role of ion migration under working conditions, we constructed a laterally structured Au/$CH_3NH_3PbI_3$/Au sample (Figure S1) for the convenience of applying an external electric field to reproduce the working conditions of the optoelectronic devices. A home-built wide-field fluorescence microscope was used to study the PL responses of the $CH_3NH_3PbI_3$ crystals under an applied electric field. With the high spatial resolution of our apparatus, we observed that two different PL responses successively happened in one local region of the crystal under an applied electric field. First, an irreversible PL quenching behavior occurred in the local region and gradually moved toward the cathode direction. Such processes were accompanied by a

Received: June 7, 2021
Accepted: July 19, 2021
Published: July 23, 2021

https://doi.org/10.1021/acs.jpclett.1c01803
J. Phys. Chem. Lett. 2021, 12, 7106–7112

permanent change of the crystal morphology. After the PL quenching of this region had entirely completed, the reversible PL response started to come out in this region. By studying the PL spectra and lifetime during the two processes and evaluating the diffusion constant from the velocity of the migrating front and the external voltage, we attributed the irreversible and reversible responses to electric field induced photo-annealing effect and the activation/deactivation of the radiative recombination center via iodine ion migration, respectively.

To investigate the effects of the applied electric field on the OMHP materials which was similar to that under working conditions, a voltage of 1 V and an excitation laser at 532 nm with 4.5 W/cm^2 were applied to the laterally structured devices for 2 min. As shown in Figure 1, a PL quenched area initially

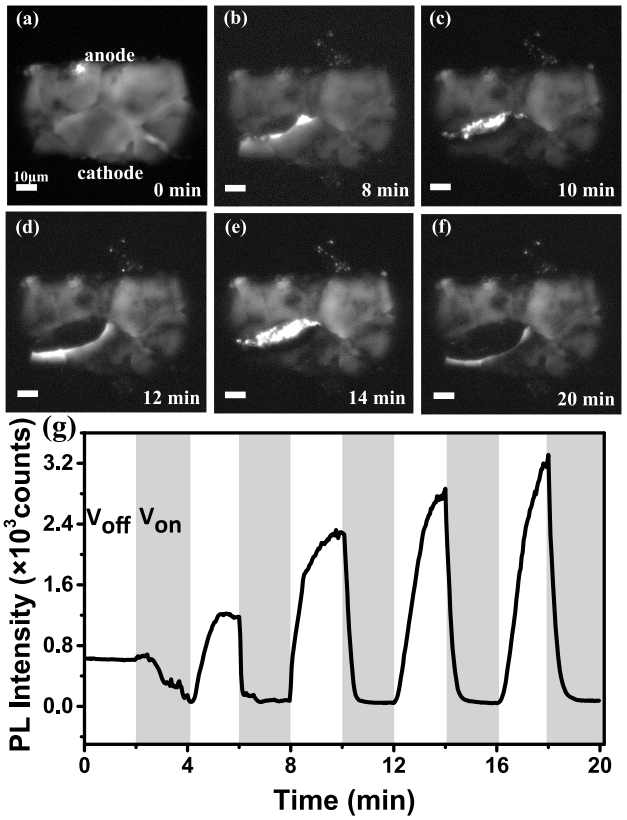

Figure 1. Observation of a quenched area advancing toward the cathode. (a–f) Time-dependent PL images of the $CH_3NH_3PbI_3$ crystals under an external applied voltage which was periodically switched between "off" and "on" for five cycles. (g) Time-resolved profiles of the PL response selected from the dark area. The applied voltage was 1 V, and the excitation power density was 4.5 W/cm^2.

formed with a bright and sharp front in the local region of the crystals. With continuously applied voltage and excitation, the front also gradually moved toward the negative electrode, and the quenched area also gradually enlarged. After the voltage was turned off, the movement of the front stopped and the PL of the dark area soon became even brighter rather than returning to the initial state. Then, upon further applying the external voltage to the $CH_3NH_3PbI_3$ crystals, the brighter area was quenched again, and the quenched processes also have a direction from the positive to negative electrode, as shown in Supplementary Movie 1. From Figure 1g we can observe that with a continuously switched on/off voltage, the PL intensity in the formed local region showed a ∼5 fold enhancement. Also, the PL quenching rate after the voltage was switched on became much faster. Because such PL behaviors still can occur when decreasing the excitation power to 0.2 W/cm^2 and the further PL enhancement/quenching behaviors under switchable applied electric field were also fully reversible under 4.5 W/cm^2 (Figure 1g), photodegradation effect can be ruled out. In addition, because the bright and sharp front formed during the first cycle was stopped when the voltage was switched off, we also tried to check if the movement of the front required the coexistence of the excitation. As shown in Figure S2, when the bright front began to move, we switched off the laser and kept the applied voltage for 20 s. The excitation was then switched on again, and the position of the front did not change and continued to diffuse after reopening the laser for 11 s. Moreover, a proportional relationship between the velocity of the front movement and excitation power (not larger than 4.5 W/cm^2) was also observed (Figure S2d), verifying that the increased excitation power less than 4.5 W/cm^2 mainly accelerated the migration of the front rather than the photodegradation. Both results indicated that formation of the first period required the coexistence of an applied electric field and photoexcitation.

For the quenched area in which the front had completely reached the negative electrode, the overall PL intensity was strong in the absence of voltage. We observed that the PL of the brightened area would be completely quenched without a migrating front when the voltage was applied again and can be later restored by removing the voltage (Figure S3). Apparently, the whole process of voltage repeat test in the completely quenched region was reversible (Supplementary Movie 2) and can also be seen from the PL intensity traces in Figure S3d. Therefore, the applied voltage induced an irreversible PL process in the area where the voltage was first applied and a reversible process when the area had entirely quenched. There were also reports of PL responses in similar lateral device architectures in the literature; however, the PL responses were progressively suppressed from the beginning of the anode to the cathode[16−18] or the opposite[23,24] upon biasing and without PL intensity enhancement when the biasing was removed.

To understand the formation mechanisms of the two different processes under applied electric field and photoexcitation, we performed detailed investigations on the processes. First, from the PL images shown in Figure 1, we can observe that the morphology no longer appeared to be a flat bulk crystal after the initial PL quenching processes happened. We carried out the SEM measurements to compare the regions with and without PL quenching processes. As shown in Figure 2a, a more striking contrast can be observed between the morphology of the quenched region and the normal region. The morphology of the quenched region was greatly changed and became coral-like in shape while the normal region almost did not change upon the application of voltage and photoexcitation. The morphology of the same $CH_3NH_3PbI_3$ sample was also presented in both SEM images and PL images for direct comparisons, as shown in Figure S4, which also proved the variation of the crystal morphology after the quenching processes. The variation of the morphology can also be reflected from the PL spectra. From Figure 2c,d, a clear blue shift of the PL can be observed during the first PL quenching process which also corresponded to the reduction of the crystal size.[25] Following this process, the applied voltage was switched off, and the PL intensity then showed an

https://doi.org/10.1021/acs.jpclett.1c01803
J. Phys. Chem. Lett. 2021, 12, 7106−7112

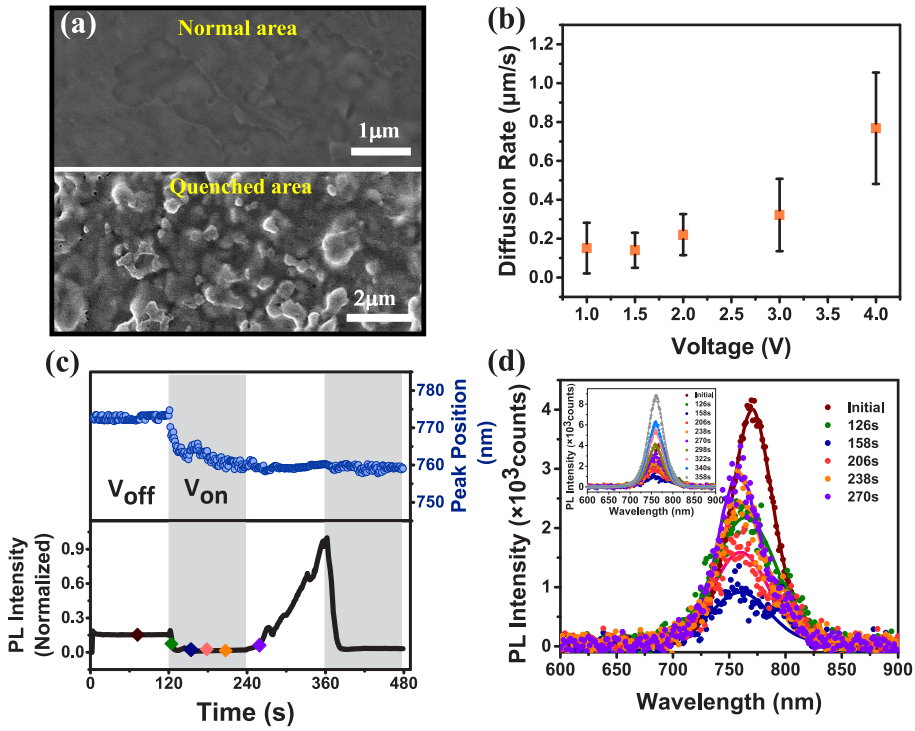

Figure 2. (a) SEM images of a normal region and a quenched region in a $CH_3NH_3PbI_3$ film. (b) Correlation between the applied voltage and the migrating front velocity. (c) PL intensity and peak position traces of the darkened region for repeat experiment when the voltage was 1 and 0 V. (d) Corresponding PL spectra at different times marked in the lower part of panel c. The inset was the variation of PL spectra within 360 s in Figure 3c.

enhancement without any shift in PL spectra. Upon further switching on of the applied voltage, although the PL quenched again, the PL spectra still can remain stable, which was different from the first process. Such a process will be discussed later. In general, we can conclude that the first electric-field-induced PL quenching process in the local region of the $CH_3NH_3PbI_3$ crystal was irreversible and must be correlated with the irreversible morphology variation observed in the crystal.

Because the first PL quenching process under applied voltage always started from one local region inside the crystal and moved along the direction from the anode to cathode, to better understand this process, we investigated the relationship between the velocity of the migrating front and the external voltage. With the applied voltage varying from 1.0 to 4.0 V, the velocity gradually increased and reached about three times the initial rate when the voltage was 4.0 V (Figure 2b). The corresponding diffusion constant D was calculated to be $(1.65 \pm 1.04) \times 10^{-13}$ m^2 s^{-1} based on the Einstein relation,[26] which was very close to the diffusion constant of $(1.0 \pm 0.4) \times 10^{-13}$ m^2 s^{-1} of iodine ions obtained by Li et al.[17] Such results suggested that the first PL quenching processes should be concerned with diffusion of iodine ions inside the crystals. In addition, the irreversible PL quenching was always accompanied by a migrating front which always showed a higher PL intensity. Thus, we suggest that there should be traps transforming from deep energy levels to shallow energy levels and then to deep energy levels corresponding to the PL intensity varying from dark to bright and then to dark. Considering the fact that the bright migration front always started from the grain boundary and the transition levels and formation energy of different traps obtained from theoretical calculations,[27] antisite defects MA_I with deep energy levels can be candidates responsible for such irreversible PL responses. The transformation processes can be described as the following: Because of the fast crystallization process, relative high concentration of antisite defects MA_I can be formed in some areas. Under an electric field, the iodine ions will migrate toward the anode direction under the electric field until reaching the boundary. The migrated iodine ions can replace the MA^+ ions in MA_I (deep energy levels) to deactivate the left V_I parts, which act as quenching sites on the surface of the $CH_3NH_3PbI_3$ crystals,[27,28] and the MA^+ ions will turn into intersitial MA_i defects (shallow energy levels). Such processes will deactivate the MA_I defects. Thus, with simultaneous photoexcitation, such areas will exhibit a PL enhancement behavior. However, continuous photoexcitation will make MA_i transform to CH_3NH_2 and evaporate. Simultaneously, the iodine ions replacing the MA^+ ions in primitive MA_I sites will be released and further migrate toward the anode producing the vacancy defect V_I on the surface of $CH_3NH_3PbI_3$ crystals, which can lead to the irreversible PL quenching behavior.[29,30] This process was named because it showed an obvious PL quenching phenomenon compared to the initial state. However, given the mechanism discussed above, it contains two processes under photoexcitation and applied electric field. One was the irreversible deactivation processes of the MA_I defects by iodine ion migration. Because irreversible deactivation can lead to the increase of the PL intensity beyond the initial state when switching off the applied electric field, this process could indicate an optimization of the OMHP crystals, which was similar to the conventional thermal annealing. Thus, such an optimization process can be viewed as a photo-annealing effect. The following process was the formation of the V_I defects by further migration of the iodine ions, which led to the PL quenching. It is worth noting that such V_I were also responsible for the second reversible PL quenching behaviors under a switchable applied electric field.

https://doi.org/10.1021/acs.jpclett.1c01803
J. Phys. Chem. Lett. 2021, 12, 7106−7112

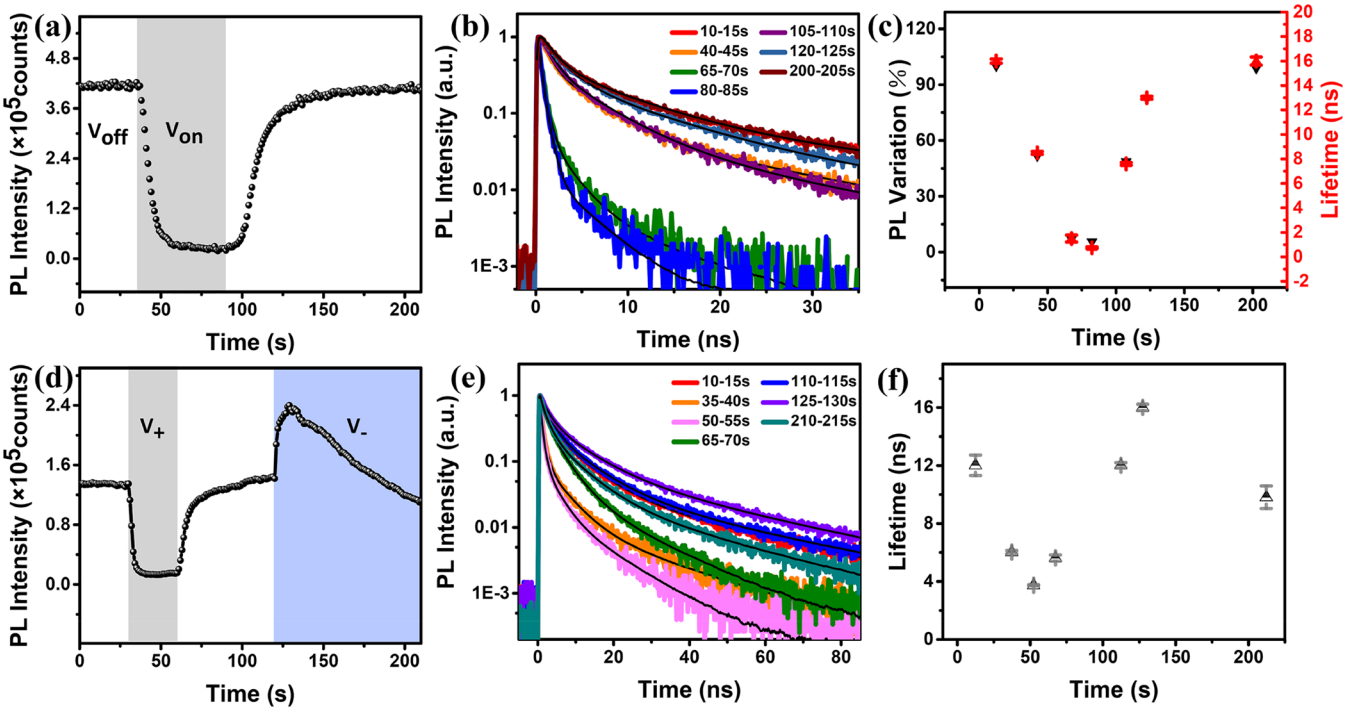

Figure 3. PL intensity traces (a) and corresponding PL lifetime (b) of the quenched area during the reversible process when the applied voltage was switched on and off. (c) PL intensity and lifetime variation compared with the initial state of panels a and b under different voltages. PL intensity traces (d) and corresponding PL lifetime (e) of the quenched area during the reversible process when the polarity of the voltage was changed. (f) Lifetime fitted from the decay traces in panel e. The applied voltage was 1 V.

In general, the electric-field-induced photo-annealing effect will trigger the following dissociation in a local region of the crystal surface:

$$CH_3NH_3PbI_3 \rightarrow PbI_2 + HI + CH_3NH_2 \quad (1)$$

The change of the crystal morphology in Figure 2a also proved the evaporation of CH_3NH_2, which induces the variation of the chemical surroundings in the quenched regions. The irreversible blue shift of the PL spectra as shown in Figure 2d can also explain the permanent modification in the quenched region. What needs to be highlighted is that the annealing process required the participation of both an applied electric field and photoexcitation. As shown in Figure S2, the movement of the front will stop once the excitation is switched off. Thus, the morphology of the crystal slowly changed as the reaction proceeded. Also, from eq 1 we can see that PbI_2 should be formed after the reaction. Merdasa et al. had found that at the interface between $PbI_2/CH_3NH_3PbI_3$, a blue-shifted PL spectra will be observed at low excitation intensity at 450 nm due to the PbI_2-enabled bimolecular recombination.[31] Thus, to prove the formation of $PbI_2/CH_3NH_3PbI_3$ interfaces inside the quenched region after the reaction, we also tried to apply a 450 nm excitation with a power density of 0.4 and 0.06 W/cm^2. As shown in Figure S5, besides the intrinsic PL peak of $CH_3NH_3PbI_3$, we can clearly see a weak peak near 660 nm proving the existence of PbI_2, which can also help to verify the emergence of the photo-annealing effect as reported in the literature.[32]

As mentioned above, a reversible PL response behavior in the same region was observed following the irreversible PL quenching processes with continuously switching on/off the applied voltage. As shown in Figure 1, the PL intensity of the local region will increase beyond the initial state once the applied voltage is switched off and then quench again after switching on the voltage. Compared to the very first PL quenching process, the quenching rate of the reversible process become faster, showing that they are two different processes. In addition, the PL morphology remained constant after several circles of the PL variation, which was also totally different from the irreversible change of the morphology in the first step. The PL spectra during this reversible quenching responses were also measured in Figure S6. No peak shift in the spectra indicates that there was no chemical or morphological change during this process. Then we measured the variation of the transient PL lifetime of the PL response under periodically applied voltage. Figure 3 shows that the variation of the lifetime was consistent with the tendency of the PL intensity, indicating the formation of traps when applying voltage to the crystals.

As reported before,[33] injected electrons or holes can help to activate or deactivate the traps inducing the PL variation. Thus, to confirm if the formation of traps was correlated with the injected electrons or holes, we also tried to change the direction of the applied electric field to observe the PL variation. However, the PL always exhibited an enhancement for a short while followed by a quenching process (Figure 3d) rather than directly showing a pure PL enhancement or PL quenching behavior. The PL lifetime in Figure 3f also coincided with the tendency of the PL variation, indicating the traps also dynamically varied after changing the direction of the electric field. To find whether such PL behavior was correlated with the direction of the electrode, we also continuously changed the electric field direction and found that this behavior will always exist whatever the direction of the electric field was from anode to cathode or the opposite, as shown in Figure S7. Thus, we believe this process was different

https://doi.org/10.1021/acs.jpclett.1c01803
J. Phys. Chem. Lett. 2021, 12, 7106−7112

from the injected electron/hole-induced PL variations. The movement of the reversible PL quenching processes always showed a tendency in the direction from anode to cathode and the recovery processes also regularly showed the opposite direction without changing the morphology of $CH_3NH_3PbI_3$ crystals as shown in Supplementary Movie 3. Combining this with the simultaneous PL dynamic variations, we propose that such a PL quenching process should also be correlated with the effect from the electric-field-induced iodine ion migration, which is responsible for the activation/deactivation of the radiative recombination centers in the local region.

From the above discussion, we assigned the two processes to be correlated with the electric-field-induced photo-annealing effect and iodine ion migration mediated trap activation/deactivation effect, respectively. Considering that the crystal morphology and quality determine the heterogeneity of the defect composition, ionic movement processes will be affected by the kinds of defects and thus exhibit different behaviors under an electric field. As a result, the reported two processes in this work, which were assigned to iodine ion migration, can be observed only in some local regions of the crystal containing the specified defect rather than all over the crystal. We suggest antisite defects MA_I should be responsible for such PL behaviors. When the external voltage was first applied to the $CH_3NH_3PbI_3$ crystal, the migration of the iodine ions near the boundary will promote the dissociation of antisite defects MA_I into MA_i and the iodine ion occupied V_I (surface) deactivating the quenching trap MA_I. Then, simultaneous photoexcitation will first induce the bright migration front, and then the photo-annealing effect will evaporate the CH_3NH_2 and release the gathering iodine ions to migrate further, permanently producing V_I (surface) on the surface of $CH_3NH_3PbI_3$ crystal, which results in the irreversible PL quenching. The second reversible PL response should be correlated with the state transformation of the V_I (surface) traps. After the applied voltage is removed, the PL intensity of the quenched region will gradually increase beyond the initial state (Figure 4). Such PL enhancement behavior should come from two contributions: (1) The back migration of iodine ions can deactivate the deep-lying energy level trap V_I (surface). (2) The reduction of the crystal size will accelerate the passivation of the defects, for example, V_I (surface) on the $CH_3NH_3PbI_3$ surface inducing the PL enhancement.[34] The former mechanism can help to make the crystal recover to the initial state, while the later can explain the superior part of the PL intensity over the initial state when switching off the electric field. The reversible PL quenching under applied voltage was always along the direction of the electric field, whereas the recovery processes without applied voltage were along the opposite way, indicating that the reversible PL response should be correlated with the migration of iodine ions. Also, the PL response which first showed an increase in the PL intensity and then followed a PL quenching process when changing the direction of the electric field can also be explained. When changing the direction, the iodine ions will first move to the opposite direction and across the primitive quenched region, which will quickly deactivate the iodine vacancies leading to the PL enhancement. Then the continuously applied voltage will drive the iodine ions to move to the new anode direction, producing iodine vacancies again leading to the PL quenching as described in Figure 4. In general, such a model can explain the phenomena existing in local regions of the $CH_3NH_3PbI_3$ crystals with the simultaneous application of applied voltage and photoexcitation.

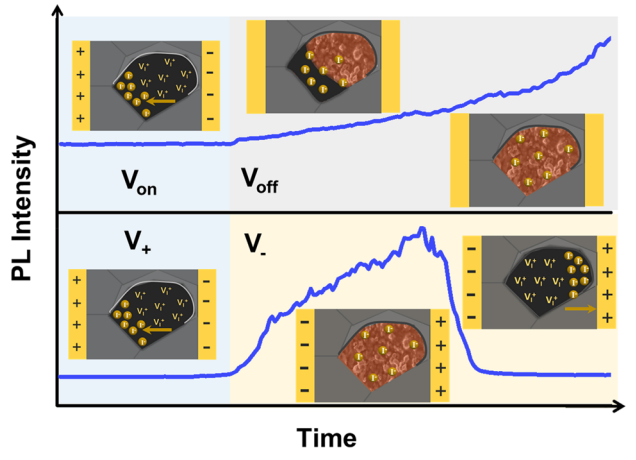

Figure 4. Schematic diagram of the influence of iodine ion migration on the quenching responses under an external electric field.

In summary, a wide-field fluorescence microscope was used to gain a thorough understanding of the dynamic processes of the ionic movement in $CH_3NH_3PbI_3$ crystals under an applied electric field. Two distinct processes were observed: One was an irreversible PL quenching accompanied by a remarkable change of the crystal morphology. The other was a reversible PL response existing when continuously switching on and off the voltage. With the spreading velocity of the quenched regions, the permanent blue shift of PL spectra during the irreversible processes, and the consistent variation degree of PL intensity and lifetimes during the reversible response, the mechanisms were attributed to electric-field-induced photo-annealing effects and iodine ion migration, respectively. This work not only revealed the synergistic optimization of the electric-field-induced photo-annealing effect but also explained the effect of the ionic movements under an applied electric field, which will greatly help us to attain deep insights into perovskite-based optoelectronic devices under working conditions as we seek effective ways to improve the efficiency of the OMHP devices.

■ ASSOCIATED CONTENT

Supporting Information

The Supporting Information is available free of charge at https://pubs.acs.org/doi/10.1021/acs.jpclett.1c01803.

Experimental methods, schematic of laterally structured sample, observation of a quenched area when the voltage was applied again, PL and SEM images of the sample that has quenched and normal areas, PL spectra of the quenched area with 450 nm excitation at low fluence, and PL spectra during the reversible process (PDF)

Movie 1: PL quenching from anode to cathode during the voltage repeat test (MP4)

Movie 2: Reversible PL quenching process in the completely quenched region (MP4)

Movie 3: PL behavior during the change of external applied voltage direction (MP4)

https://doi.org/10.1021/acs.jpclett.1c01803
J. Phys. Chem. Lett. 2021, 12, 7106−7112

AUTHOR INFORMATION

Corresponding Authors

Daocheng Hong − *Key Laboratory for Advanced Technology in Environmental Protection of Jiangsu Province, Yancheng Institute of Technology, Yancheng, Jiangsu 224051, China;* orcid.org/0000-0003-2193-8260; Email: hdaocheng@gmail.com

Yuxi Tian − *Key Laboratory of Mesoscopic Chemistry of MOE, School of Chemistry and Chemical Engineering, Nanjing University, Nanjing, Jiangsu 210023, China*; Email: tyx@nju.edu.cn

Authors

Yu Du − *Key Laboratory of Mesoscopic Chemistry of MOE, School of Chemistry and Chemical Engineering, Nanjing University, Nanjing, Jiangsu 210023, China;* orcid.org/0000-0003-2360-3739

Sushu Wan − *Key Laboratory of Mesoscopic Chemistry of MOE, School of Chemistry and Chemical Engineering, Nanjing University, Nanjing, Jiangsu 210023, China;* orcid.org/0000-0001-8666-9255

Mingcai Xie − *Key Laboratory of Mesoscopic Chemistry of MOE, School of Chemistry and Chemical Engineering, Nanjing University, Nanjing, Jiangsu 210023, China*

Yuren Xia − *Key Laboratory of Mesoscopic Chemistry of MOE, School of Chemistry and Chemical Engineering, Nanjing University, Nanjing, Jiangsu 210023, China*

Weiqing Yang − *Key Laboratory of Mesoscopic Chemistry of MOE, School of Chemistry and Chemical Engineering, Nanjing University, Nanjing, Jiangsu 210023, China*

Zhihong Wei − *Key Laboratory of Mesoscopic Chemistry of MOE, School of Chemistry and Chemical Engineering, Nanjing University, Nanjing, Jiangsu 210023, China*

Yajie Zhu − *Key Laboratory of Mesoscopic Chemistry of MOE, School of Chemistry and Chemical Engineering, Nanjing University, Nanjing, Jiangsu 210023, China*

Yan Hua − *Key Laboratory of Mesoscopic Chemistry of MOE, School of Chemistry and Chemical Engineering, Nanjing University, Nanjing, Jiangsu 210023, China;* orcid.org/0000-0003-1732-8646

Zhong Jin − *Key Laboratory of Mesoscopic Chemistry of MOE, School of Chemistry and Chemical Engineering, Nanjing University, Nanjing, Jiangsu 210023, China;* orcid.org/0000-0001-8860-8579

Complete contact information is available at: https://pubs.acs.org/10.1021/acs.jpclett.1c01803

Notes

The authors declare no competing financial interest.

ACKNOWLEDGMENTS

This work is supported by National Natural Science Foundation of China (NSFC Nos. 22073046 and 62011530133) and the Fundamental Research Funds for the Central Universities (020514380256).

REFERENCES

(1) Wang, K.; Yang, D.; Wu, C.; Sanghadasa, M.; Priya, S. Recent Progress in Fundamental Understanding of Halide Perovskite Semiconductors. *Prog. Mater. Sci.* **2019**, *106*, 100580.

(2) National Renewable Energy Laboratory (NREL). Best Research-Cell Efficiency Chart. https://www.nrel.gov/pv/cell-efficiency.html (accessed 2021-03-30).

(3) Wang, R.; Mujahid, M.; Duan, Y.; Wang, Z.; Xue, J.; Yang, Y. A Review of Perovskites Solar Cell Stability. *Adv. Funct. Mater.* **2019**, *29* (47), 1808843.

(4) Sun, Q.; Fassl, P.; Becker-Koch, D.; Bausch, A.; Rivkin, B.; Bai, S.; Hopkinson, P. E.; Snaith, H. J.; Vaynzof, Y. Role of Microstructure in Oxygen Induced Photodegradation of Methylammonium Lead Triiodide Perovskite Films. *Adv. Energy Mater.* **2017**, *7* (20), 1700977.

(5) van Reenen, S.; Kemerink, M.; Snaith, H. J. Modeling Anomalous Hysteresis in Perovskite Solar Cells. *J. Phys. Chem. Lett.* **2015**, *6* (19), 3808−3814.

(6) Chen, B.; Yang, M.; Priya, S.; Zhu, K. Origin of J-V Hysteresis in Perovskite Solar Cells. *J. Phys. Chem. Lett.* **2016**, *7* (5), 905−917.

(7) Elumalai, N. K.; Uddin, A. Hysteresis in Organic-Inorganic Hybrid Perovskite Solar Cells. *Sol. Energy Mater. Sol. Cells* **2016**, *157*, 476−509.

(8) O'Regan, B. C.; Barnes, P. R. F.; Li, X.; Law, C.; Palomares, E.; Marin-Beloqui, J. M. Optoelectronic Studies of Methylammonium Lead Iodide Perovskite Solar Cells with Mesoporous TiO_2: Separation of Electronic and Chemical Charge Storage, Understanding Two Recombination Lifetimes, and the Evolution of Band Offsets during J-V Hysteresis. *J. Am. Chem. Soc.* **2015**, *137* (15), 5087−5099.

(9) Miyano, K.; Yanagida, M.; Tripathi, N.; Shirai, Y. Hysteresis, Stability, and Ion Migration in Lead Halide Perovskite Photovoltaics. *J. Phys. Chem. Lett.* **2016**, *7* (12), 2240−2245.

(10) Zhang, T.; Meng, X.; Bai, Y.; Xiao, S.; Hu, C.; Yang, Y.; Chen, H.; Yang, S. Profiling the Organic Cation-Dependent Degradation of Organolead Halide Perovskite Solar Cells. *J. Mater. Chem. A* **2017**, *5* (3), 1103−1111.

(11) Besleaga, C.; Abramiuc, L. E.; Stancu, V.; Tomulescu, A. G.; Sima, M.; Trinca, L.; Plugaru, N.; Pintilie, L.; Nemnes, G. A.; Iliescu, M.; et al. Iodine Migration and Degradation of Perovskite Solar Cells Enhanced by Metallic Electrodes. *J. Phys. Chem. Lett.* **2016**, *7* (24), 5168−5175.

(12) Tress, W.; Marinova, N.; Moehl, T.; Zakeeruddin, S. M.; Nazeeruddin, M. K.; Grätzel, M. Understanding the Rate-Dependent J-V Hysteresis, Slow Time Component, and Aging in $CH_3NH_3PbI_3$ Perovskite Solar Cells: The Role of a Compensated Electric Field. *Energy Environ. Sci.* **2015**, *8* (3), 995−1004.

(13) Calado, P.; Telford, A. M.; Bryant, D.; Li, X.; Nelson, J.; O'Regan, B. C.; Barnes, P. R. F. Evidence for Ion Migration in Hybrid Perovskite Solar Cells with Minimal Hysteresis. *Nat. Commun.* **2016**, *7* (1), 13831.

(14) Kang, D.; Park, N. On the Current-Voltage Hysteresis in Perovskite Solar Cells : Dependence on Perovskite Composition and Methods to Remove Hysteresis. *Adv. Mater.* **2019**, *31* (34), 1805214.

(15) Yuan, Y.; Wang, Q.; Shao, Y.; Lu, H.; Li, T.; Gruverman, A.; Huang, J. Electric-Field-Driven Reversible Conversion Between Methylammonium Lead Triiodide Perovskites and Lead Iodide at Elevated Temperatures. *Adv. Energy Mater.* **2016**, *6* (2), 1501803.

(16) Deng, X.; Wen, X.; Lau, C. F. J.; Young, T.; Yun, J.; Green, M. A.; Huang, S.; Ho-Baillie, A. W. Y. Electric Field Induced Reversible and Irreversible Photoluminescence Responses in Methylammonium Lead Iodide Perovskite. *J. Mater. Chem. C* **2016**, *4* (38), 9060−9068.

(17) Li, C.; Guerrero, A.; Zhong, Y.; Gräser, A.; Luna, C. A. M.; Köhler, J.; Bisquert, J.; Hildner, R.; Huettner, S. Real-Time Observation of Iodide Ion Migration in Methylammonium Lead Halide Perovskites. *Small* **2017**, *13* (42), 1701711.

(18) Chen, S.; Wen, X.; Sheng, R.; Huang, S.; Deng, X.; Green, M. A.; Ho-Baillie, A. Mobile Ion Induced Slow Carrier Dynamics in Organic-Inorganic Perovskite $CH_3NH_3PbBr_3$. *ACS Appl. Mater. Interfaces* **2016**, *8* (8), 5351−5357.

(19) Kim, S.-G.; Li, C.; Guerrero, A.; Yang, J.-M.; Zhong, Y.; Bisquert, J.; Huettner, S.; Park, N.-G. Potassium Ions as a Kinetic Controller in Ionic Double Layers for Hysteresis-Free Perovskite Solar Cells. *J. Mater. Chem. A* **2019**, *7* (32), 18807−18815.

(20) Li, C.; Guerrero, A.; Huettner, S.; Bisquert, J. Unravelling the Role of Vacancies in Lead Halide Perovskite through Electrical Switching of Photoluminescence. *Nat. Commun.* **2018**, *9* (1), 5113.

(21) Phung, N.; Al-Ashouri, A.; Meloni, S.; Mattoni, A.; Albrecht, S.; Unger, E. L.; Merdasa, A.; Abate, A. The Role of Grain Boundaries on Ionic Defect Migration in Metal Halide Perovskites. *Adv. Energy Mater.* **2020**, *10* (20), 1903735.
(22) Hu, X.; Wang, X.; Fan, P.; Li, Y.; Zhang, X.; Liu, Q.; Zheng, W.; Xu, G.; Wang, X.; Zhu, X.; et al. Visualizing Carrier Transport in Metal Halide Perovskite Nanoplates via Electric Field Modulated Photoluminescence Imaging. *Nano Lett.* **2018**, *18* (5), 3024−3031.
(23) Jacobs, D. L.; Scarpulla, M. A.; Wang, C.; Bunes, B. R.; Zang, L. Voltage-Induced Transients in Methylammonium Lead Triiodide Probed by Dynamic Photoluminescence Spectroscopy. *J. Phys. Chem. C* **2016**, *120* (15), 7893−7902.
(24) Birkhold, S. T.; Precht, J. T.; Liu, H.; Giridharagopal, R.; Eperon, G. E.; Schmidt-Mende, L.; Li, X.; Ginger, D. S. Interplay of Mobile Ions and Injected Carriers Creates Recombination Centers in Metal Halide Perovskites under Bias. *ACS Energy Lett.* **2018**, *3* (6), 1279−1286.
(25) Tian, Y.; Merdasa, A.; Unger, E.; Abdellah, M.; Zheng, K.; McKibbin, S.; Mikkelsen, A.; Pullerits, T.; Yartsev, A.; Sundström, V.; et al. Enhanced Organo-Metal Halide Perovskite Photoluminescence from Nanosized Defect-Free Crystallites and Emitting Sites. *J. Phys. Chem. Lett.* **2015**, *6* (20), 4171−4177.
(26) Sandberg, O. J.; Zeiske, S.; Zarrabi, N.; Meredith, P.; Armin, A. Charge Carrier Transport and Generation via Trap-Mediated Optical Release in Organic Semiconductor Devices. *Phys. Rev. Lett.* **2020**, *124* (12), 128001.
(27) Shan, W.; Saidi, W. A. Segregation of Native Defects to the Grain Boundaries in Methylammonium Lead Iodide Perovskite. *J. Phys. Chem. Lett.* **2017**, *8* (23), 5935−5942.
(28) Yin, W.-J.; Shi, T.; Yan, Y. Unique Properties of Halide Perovskites as Possible Origins of the Superior Solar Cell Performance. *Adv. Mater.* **2014**, *26* (27), 4653−4658.
(29) Zhou, Y.; Hu, X.; Xie, D.; Tian, Y. Mechanisms of Oxygen Passivation on Surface Defects in $MAPbI_3$ Revealed by First-Principles Study. *J. Phys. Chem. C* **2020**, *124* (6), 3731−3737.
(30) Hong, D.; Zhou, Y.; Wan, S.; Hu, X.; Xie, D.; Tian, Y. Nature of Photoinduced Quenching Traps in Methylammonium Lead Triiodide Perovskite Revealed by Reversible Photoluminescence Decline. *ACS Photonics* **2018**, *5* (5), 2034−2043.
(31) Merdasa, A.; Kiligaridis, A.; Rehermann, C.; Abdi-Jalebi, M.; Stöber, J.; Louis, B.; Gerhard, M.; Stranks, S. D.; Unger, E. L.; Scheblykin, I. G. Impact of Excess Lead Iodide on the Recombination Kinetics in Metal Halide Perovskites. *ACS Energy Lett.* **2019**, *4* (6), 1370−1378.
(32) Wang, D.; Wu, C.; Luo, W.; Guo, X.; Qi, X.; Zhang, Y.; Zhang, Z.; Zhu, N.; Qu, B.; Xiao, L.; et al. To Greatly Reduce Defects via Photoannealing for High-Quality Perovskite Films. *ACS Appl. Mater. Interfaces* **2019**, *11* (23), 20943−20948.
(33) Du, Y.; Wan, S.; Pan, Y.; Xie, M.; Ding, M.; Hong, D.; Tian, Y. Deactivation/Activation of Quenching Defects in $CH_3NH_3PbI_3$ Perovskite by Direct Electron Injection/Extraction. *J. Phys. Chem. Lett.* **2021**, *12* (2), 773−780.
(34) Tian, Y.; Peter, M.; Unger, E.; Abdellah, M.; Zheng, K.; Pullerits, T.; Yartsev, A.; Sundström, V.; Scheblykin, I. G. Mechanistic Insights into Perovskite Photoluminescence Enhancement: Light Curing with Oxygen Can Boost Yield Thousandfold. *Phys. Chem. Chem. Phys.* **2015**, *17* (38), 24978−24987.

https://doi.org/10.1021/acs.jpclett.1c01803
J. Phys. Chem. Lett. 2021, 12, 7106−7112